

The INCA Icing Potential

Alexander Kann, Thomas Haiden and Klaus von der Emde
Central Institute for Meteorology and Geodynamics
Hohe Warte 38, A-1190 Vienna, Austria, alexander.kann@zamg.ac.at

Abstract — An icing potential developed in the framework of INCA (Integrated Nowcasting Through Comprehensive Analysis) represents the Austrian contribution to the COST-727 action “Measuring and Forecasting Atmospheric Icing on Structures”. The system is based on a NWP model as a first guess and corrects these forecasts by observations. Besides a large set of surface fields, it provides 3D analyses and forecasts of temperature, humidity and wind which are used as input for the parameterization of the icing module. With respect to the predictability of the phenomenon “icing” in general, a potential or probability is calculated instead of quantitative amounts of ice loads. The paper shortly describes the INCA analysis and forecasting system with special emphasis on temperature, humidity and wind. The parameterization of the icing potential is introduced and illustrated with examples. Some considerations about refinements of the parameterization are given, followed by concluding remarks.

I. INTRODUCTION

The INCA analysis and nowcasting system, which is in operation at ZAMG (Central Institute for Meteorology and Geodynamics), provides improved numerical forecasts especially in the nowcasting range on a very high resolution (1km x 1km). An experimental numerical product for the analysis and forecasting of an icing potential has been developed. This parameterization of in-cloud icing is empirically based on the near surface variables 2-m temperature, 2-m relative humidity and 10-m wind speed. At this experimental stage, no quantitative analysis or forecast of ice loads is implemented. However, the probability of the occurrence of an icing event is a first attempt to a quantitative approach and reflects the high degree of complexity of the phenomenon. In Section 2, the characteristics of the INCA system in general and of the 3D variables temperature, humidity and wind in particular are presented. The parameterization of the icing potential itself is highlighted in Section 3 and the subsequent Section discusses some calibration issues of the parameterization. Finally, some remarks and considerations about further work conclude this paper.

II. THE INCA SYSTEM

The INCA system, which is under continuous development at ZAMG, performs analyses of 2D and 3D fields on a 600 km x 350 km grid at 1 km x 1 km horizontal resolution centered over Austria (Fig. 1). In the vertical, z-coordinates are used where z denotes the height above the ‘valley floor surface’.

This base height reflects the reference elevation in the mountainous regions and converges to the topography over flat terrain. In the current operational implementation, the temperature and humidity analyses cover the lowest 4000 meters of the atmosphere with $\Delta z=200m$. For wind, $\Delta z=125m$ and the valley floor surface is set to zero (thus, real z-coordinates are used).

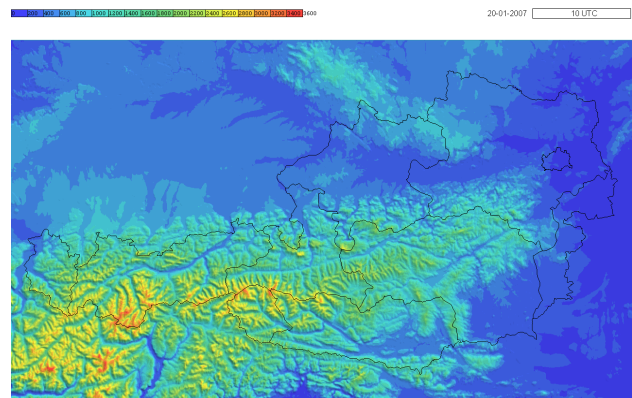


Fig. 1: INCA topography. The horizontal resolution is 1 km.

The three-dimensional analyses of temperature, humidity and wind are based on NWP forecast fields as a first guess and superimposed observations to correct them. In the operational implementation, the deterministic limited area model ALADIN-AUSTRIA is used which runs on 9.6 km horizontal resolution with 60 vertical levels (Wang et al. 2006). ZAMG operates about 250 automated weather stations (Teilautomatisches Wetterstationsnetz, TAWES) in Austria. Additionally, stations from the hydrological network are integrated into the system.

The temperature (and humidity) analyses are constructed in the following way: The first guess of the ALADIN-AUSTRIA forecast is interpolated tri-linearly onto the INCA grid. As the topography of the NWP model differs from the INCA topography to a large extent, the boundary layer atmosphere from the model is shifted downwards to the INCA valley surface floor. A most unstable gradient is defined to avoid unrealistic extrapolations in cases of strong surface or elevated inversions (Haiden et al. 2009). Next, differences between the model output and observation are applied in order to correct the first guess at station location. The ALADIN-AUSTRIA temperature forecast is separated into a 2D and 3D model part:

$$T^{ALA} = TL^{ALA} + DT^{ALA} \quad (1)$$

T^{ALA} is the 2-m temperature of ALADIN-AUSTRIA; TL^{ALA} denotes the temperature at the lowest model level, and DT^{ALA} their difference. Analogously, the corrections of the first guess field are separated into a 2D (ΔTL) and 3D (ΔDT) component:

$$\Delta T = \Delta TL + \Delta DT \quad (2)$$

The 3D-contribution of the correction at station k is derived from

$$\Delta TL_k = \max[0, T_k^{OBS} - \max(TL_k^{ALA} + I_{SFC,k} DT_k^{ALA}, TL_k^{ALA} + I_{SFC,k} DT_{SCALE})], \quad (3)$$

if $T_k^{OBS} \geq TL_k^{ALA}$,

and from

$$\Delta TL_k = \min[0, T_k^{OBS} - \min(TL_k^{ALA} + I_{SFC,k} DT_k^{ALA}, TL_k^{ALA} - I_{SFC,k} DT_{SCALE})], \quad (4)$$

if $T_k^{OBS} < TL_k^{ALA}$.

The factor $I_{SFC,k}$ denotes the surface layer index and takes the values 0 at mountain slopes and tops and 1 in valleys or flat terrain. The 3D corrections ΔTL_k are then spatially interpolated onto the INCA grid by using geometrical distance weighting in the horizontal and a distance weighting in potential temperature space in the vertical. Using the three-dimensional squared 'distance' r_{ijmk}^2 between INCA grid point (i, j, m) and the k -th station, the temperature difference field at grid point (i, j, m) is obtained from the weighted average (with $n=6$ representing the number of nearest stations to the actual grid point):

$$\Delta TL(i, j, m) = \frac{\sum_{k=1}^n \frac{\Delta TL_k}{r_{ijmk}^2}}{\sum_{k=1}^n \frac{1}{r_{ijmk}^2}} \quad (5)$$

Finally, this difference field is added to the ALADIN-AUSTRIA first guess field:

$$TL^{INCA}(i, j, m) = TL^{ALA}(i, j, m) + \Delta TL(i, j, m) \quad (6)$$

Evaluation shows that the analysis error (gained by cross-validation) is less than 1 K in well-mixed situations and between 1 K and 1.5 K in stable cases.

3D-Humidity analyses are performed in an analogous way. The wind analysis is constructed similarly by a first guess of the NWP model (ALADIN-AUSTRIA), a 2D (10-m wind vector) and 3D (lowest model level wind vector) component. A factor f_{10} which varies from 0.75 in valleys and flat regions to 0.9 on exposed regions translates a 10-m wind to a model level wind. As the corrected INCA analysis wind field is not mass-consistent, an iterative relaxation algorithm is applied to satisfy this requirement. Up to now, the downscaling is purely kinematic, so no additional dynamical features besides the ones already originating from the NWP model are introduced.

The INCA forecasting system takes into account the local NWP error and merges into the NWP forecast through a prescribed weighting function. In case of temperature, model

errors are highly correlated with errors in cloudiness forecasts which lead to errors in the energy budget. Thus, the nowcasting temperature for time t_i is calculated from the relation:

$$T_{INCA}(t_i) = T_{INCA}(t_{i-1}) + f_T [T_{ALADIN}(t_i) - T_{ALADIN}(t_{i-1})], \quad (7)$$

where the factor f_T is related to the cloudiness error C_{ERR} through

$$f_T = 1 + c_N C_{ERR} \quad (8)$$

where the coefficient c_N is found typically in the range of 0.5 to 0.7.

From (7) follows, that a perfect cloudiness forecast results in a predicted temperature change which is equal to the one by the NWP model. Finally, the nowcasting temperature converges to the bias-corrected ALADIN-AUSTRIA forecast in the form of negative-exponential weighting:

$$T_{INCA}^*(t_i) = g T_{INCA}(t_i) + (1-g) T_{ALADIN}(t_i) \quad (9)$$

with

$$g(t_i) = \exp\left(-\frac{t_i - \tau_C}{\tau_D}\right) \quad (10)$$

for times $t_i > \tau_C$ and $\tau_D = 6$ hours.

The dependency of time scale τ_C on the static stability accounts for observed variations of error persistency under different synoptic situations. For example, in case of inversions, τ_C can reach values up to 12 hours.

Fig. 2 shows verification results of the INCA 2-m temperature compared to persistence and ALADIN-AUSTRIA forecast for an 18-month period.

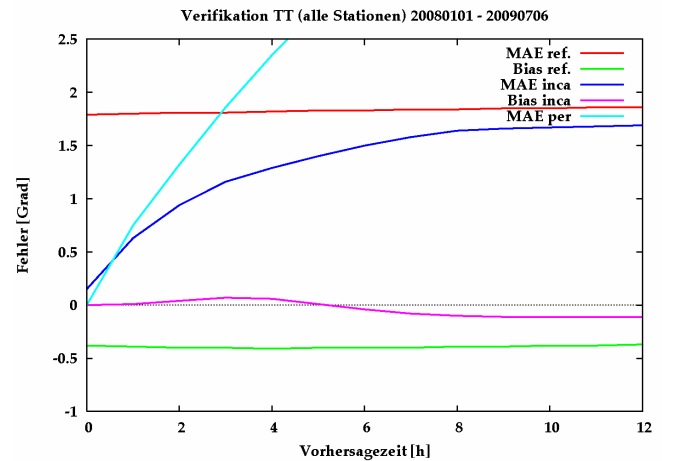


Fig. 2: Mean absolute error (MAE) and mean error (BIAS) of the INCA 2-m temperature forecast (MAE: dark blue, BIAS: purple) compared with persistency (light blue) and ALADIN-AUSTRIA (MAE: red, BIAS: green) forecast.

Averaged over all stations, typical mean absolute errors are ranging from 1 K (for +2 hours lead time) up to 1.7 K (for +12 hours lead time). Note that the MAE of INCA is still lower than the one of ALADIN-AUSTRIA at longer lead times due to application of a bias correction.

In case of wind, the three-dimensional wind vector is given by

$$\vec{v}_{INCA}(t_i) = g \vec{v}_{INCA}(t_0) + (1-g) \vec{v}_{ALADIN}(t_i) \quad (11)$$

with the weighting function:

$$g(t_i) = \max\left(1 - \frac{t_i}{\tau_v}, 0\right) \quad (12)$$

and with $\tau_v=6$ hours.

III. THE INCA ICING MODULE

An empirical parameterization for the analysis and forecasting of icing is being developed in the framework of COST-727. The icing potential reflects the rate of icing to be expected on structures due to contact freezing of supercooled cloud droplets. Icing is most likely at temperatures between 0°C and -20°C and increases with cloud water content and wind speed. Due to the lack of a liquid water variable in INCA, relative humidity is used as a substitute for identifying regions within a cloud. Temperature is used to qualitatively capture the decreasing amount of cloud liquid water in colder clouds. Formally, the icing potential IP can be written as:

$$IP = 100 \cdot f_1(T) f_2(u) f_3(h) \quad (13)$$

The functions for temperature T , wind speed u and relative humidity h are given by:

$$f_1(T) = \begin{cases} \exp[(T - T_{OPT2})/T_{SCALE}] & T < T_{OPT2} \\ 1 & T_{OPT2} \leq T < T_{OPT1} \\ T/T_{OPT1} & T_{OPT1} \leq T < T_0 \\ 0 & T \geq T_0 \end{cases} \quad (14)$$

$$f_2(u) = \min(1, u/(a(u_{MAX})^{\frac{1}{a}})) \quad (15)$$

$$f_3(h) = \min\left[1, \max\left(0, \frac{h - h_{MIN}}{h_{MAX} - h_{MIN}}\right)\right] \quad (16)$$

The rate of icing is assumed to increase linearly with wind speed up to a maximum wind speed above which the breaking off of ice becomes a limiting factor. The parameters are currently set to the following values: $T_0=0^\circ\text{C}$; $T_{OPT1}=-3^\circ\text{C}$; $T_{OPT2}=-20^\circ\text{C}$; $T_{SCALE}=10\text{K}$; $u_{max}=25\text{m s}^{-1}$; $h_{min}=95\%$; $h_{max}=100\%$, $a=1$.

Figure 3 (A-D) shows the analyzed input fields (temperature, humidity and wind speed) and the derived icing potential (probability) at 0600 UTC, 30 January 2009.

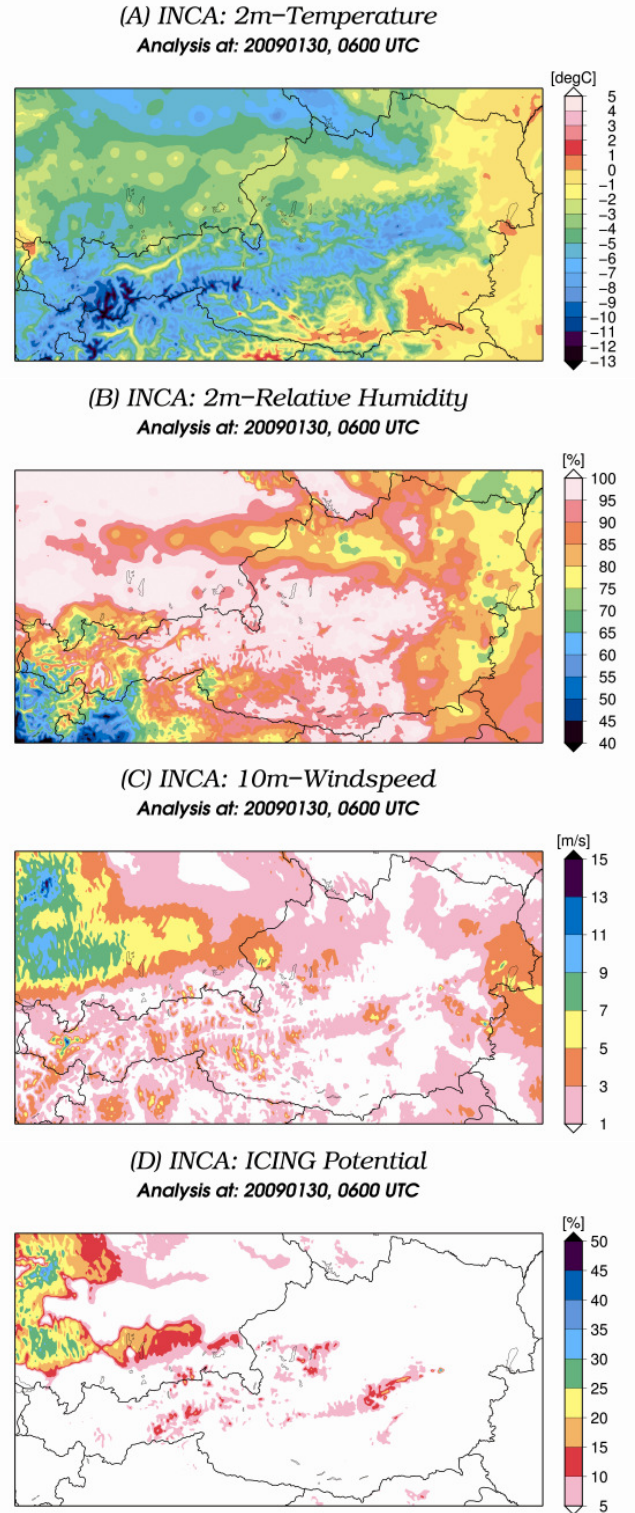


Fig. 3: INCA 2-m temperature (A), 2-m relative humidity (B), 10-m wind speed (C) and icing potential (D) analyses at 0600 UTC, 30 January 2009.

IV. REFINEMENTS OF THE ICING PARAMETERIZATION

The parameterization given in (13) to (16) is validated for Zinnwald station using standard meteorological measurements (2-m temperature, 2-m relative humidity and 10-m wind speed) and measurements of ice masses (instruments COMBITECH and EAG 200) which have been installed in the framework of the COST-727 action. The temporal distribution of the derived icing probability corresponds qualitatively well to the ice mass measurements, although probabilities in general tend to be too low (Fig. 4). Comparing the derived icing potential with the input parameters temperature, relative humidity and wind speed proves that the icing probability is highly correlated to wind speed as long as temperature and relative humidity favor the development of icing (below zero and close to saturation, Fig. 5).

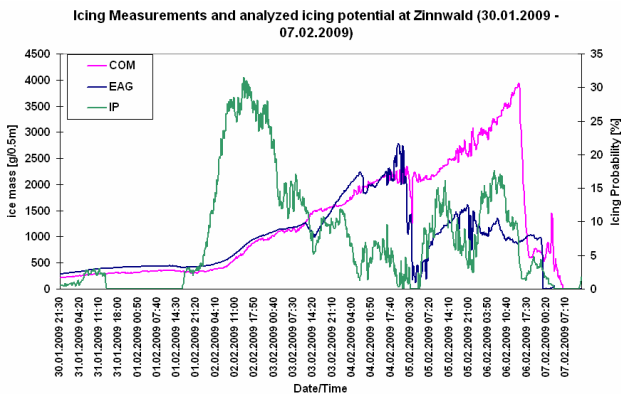


Fig. 4: Measurements of ice mass [g] of COMBITECH (purple), EAG 200 (blue) and the analysed icing potential (green) for a 1-week icing episode in winter 2009.

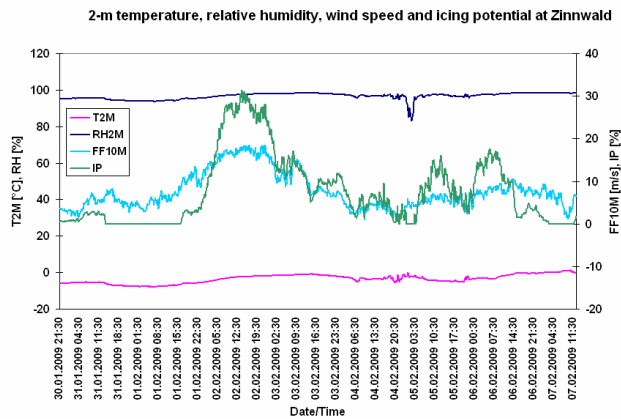


Fig. 5: 2-m temperature (purple), 2-m relative humidity (dark blue), 10-m wind speed (light blue) and icing potential (green) for a 1-week icing episode in winter 2009.

Thus, the influence of wind speed has been utilized for tuning the icing parameterization. Setting $a=2$ in (15) increases the influence of wind speed in such a way that higher probabilities are also allowed in case of lower wind speed without losing the properties of the linear increase of icing probabilities with increasing wind speed.

In Fig. 6, the INCA icing potential is illustrated for the modified parameterization (for the same case as in Fig. 3).

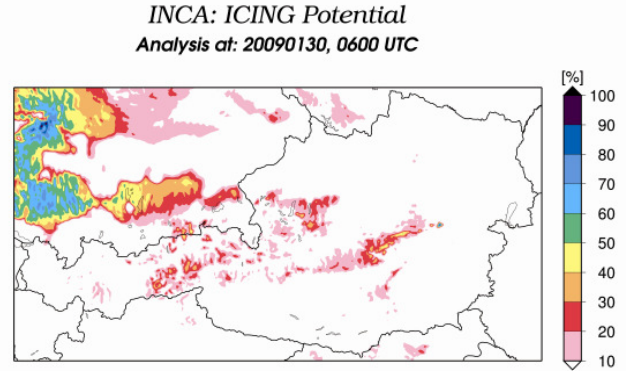


Fig. 6: Modified INCA icing potential analysis at 0600 UTC, 30 January 2009.

Especially in the western parts of the domain the icing probability reaches higher values that reflect the influence of temperature, humidity and in particular wind speed. It has to be further investigated if the improvements of the analysis at the Zinnwald station can be generalized to an improved spatial distribution of icing probabilities.

Icing data (mainly camera images) from the Guetsch station in Switzerland have been explored as well, but due to their limited quality, these data did not contribute to an improved icing parameterization.

V. CONCLUDING REMARKS

In the framework of the COST-727 action, an icing potential has been implemented in INCA. The probability of the occurrence of icing on structures is provided which is useful on a very high resolution, especially in complex terrain. The parameterization has been adapted by the use of icing measurements at Zinnwald station which finally has lead to qualitatively improved analyses.

However, the limited availability of icing measurement data hampers the development of further improvements of the icing analysis and forecast. Evaluation of the analysis algorithm and verification of the forecasts as well as measurements used for calibration issues play an essential role in the chain of improved techniques. It has to be checked carefully, if the icing measurements are able to fulfill these requirements in the near future in order to systematically review the system.

VI. ACKNOWLEDGEMENTS

The authors are thankful to the Deutscher Wetterdienst (DWD) and especially Bodo Wichura for providing the data at Zinnwald station. Thanks to Rene Cattin for providing data at Guetsch station and for fruitful discussions.

VII. REFERENCES

- [1] Y. Wang, T. Haiden, and A. Kann, "The operational Limited Area Model at ZAMG: ALADIN-AUSTRIA. *Österr. Beiträge zu Meteorologie und Geophysik*, 37.
- [2] T. Haiden, A. Kann, G. Pistotnik, K. Stadlbacher, and C. Wittmann, "Integrated Nowcasting through Comprehensive Analysis (INCA)", System description, ZAMG Rep., Feb. 2009. [Online]. Available: http://www.zamg.ac.at/fix/INCA_system.pdf